

RSC Advances



This is an *Accepted Manuscript*, which has been through the Royal Society of Chemistry peer review process and has been accepted for publication.

Accepted Manuscripts are published online shortly after acceptance, before technical editing, formatting and proof reading. Using this free service, authors can make their results available to the community, in citable form, before we publish the edited article. This *Accepted Manuscript* will be replaced by the edited, formatted and paginated article as soon as this is available.

You can find more information about *Accepted Manuscripts* in the [Information for Authors](#).

Please note that technical editing may introduce minor changes to the text and/or graphics, which may alter content. The journal's standard [Terms & Conditions](#) and the [Ethical guidelines](#) still apply. In no event shall the Royal Society of Chemistry be held responsible for any errors or omissions in this *Accepted Manuscript* or any consequences arising from the use of any information it contains.

ARTICLE

Adsorption behaviour of gluten hydrolysate on mild steel in 1M HCl and its role as a green corrosion inhibitor

Cite this: DOI: 10.1039/x0xx00000x

Pialee Roy,¹ Tarunesh Maji,¹ Sukalpa Dey,² Dipankar Sukul^{1*}

Received 00th January 2013,
Accepted 00th January 2013

DOI: 10.1039/x0xx00000x

www.rsc.org/

Search for commercially available and low cost green corrosion inhibitor in combating metal corrosion has incited to investigate the adsorption behavior and inhibition potentiality of gluten hydrolysate towards mild steel in 1 M HCl employing both electrochemical and weight loss techniques. Acting as a mixed-type inhibitor, gluten hydrolysate forms an inhibitive layer on metal enhancing polarization resistance. Thermodynamic and activation parameters for adsorption are explained following competitive physical and chemical adsorption model depending on concentration as well as temperature. FTIR data indicates involvement of amide groups, as well as side chains of amino acid residues during adsorption, while confirmatory evidence of enhanced corrosion resistance is obtained from SEM images.

Introduction

Combating corrosion of metals in different aggressive environment using inorganic and organic based inhibitors has a long history.¹⁻⁸ In many commercial inhibitor formulation, inorganic and organic inhibitors are used together, in addition to other additives, like stabilizer etc.^{2,8} But, in recent years, use of such heavy metal ion based inhibitors are getting restricted due to their environmental hazardous characteristics.⁹ Organic inhibitors may also be toxic; otherwise their synthetic process may be responsible for environmental degradation to various extent. In this regard, use of biodegradable and inexpensive green corrosion inhibitors, derived from different plant sources may be the most viable alternative.¹⁰⁻¹² Search for biocompatible corrosion inhibitors prompted researchers to investigate the efficacy of different amino acids,¹³ polysaccharides,¹⁴ vitamins,¹⁵ drug molecules,¹⁶ proteins,¹⁷ as well as numerous plant extracts.¹⁸

From our group, we have earlier demonstrated that polysaccharides in presence of thiourea impart synergistic influence towards corrosion inhibition of mild steel in acid.¹⁹ Chemical modification of polysaccharides also enhances their anti-corrosive potentiality.²⁰ Water-insoluble protein, zein in SDS micellar media has been established as a good corrosion inhibitor.²¹ In continuing this endeavor, in the present work, we have tested the adsorption characteristics of bioactive and inexpensive hydrolysate of a water soluble protein, gluten on mild steel in 1M HCl as a function of temperature and subsequently its corrosion inhibition propensity.

Gluten, a plant protein, is found in various cereal grains, like wheat, maize, barley, oats, and others.²²⁻²⁸ It is insoluble in water, but can absorb water twice than its dry weight. This unique property has made it suitable for wide use in various food industries, particularly bakery, over many centuries.²²⁻²⁵ It is reported to be safe for use as a plant protein source in aquaculture feeds²⁶, as well as in food for the pets like cats.²⁷ Different non-food applications of gluten are attributed to its thermoplasticity and good film forming ability.²³⁻²⁵ But, water insolubility has restricted its use for many potential applications. Recently, gluten is being hydrolyzed by the action of enzymes, and these water soluble hydrolysates have found versatile biological applications, including as anti-oxidants.²³⁻²⁵ Different peptide fractions of

¹Department of Chemistry, National Institute of Technology, Durgapur, West Bengal, 713209, India.

²Dr B C Roy Engineering College, Durgapur, West Bengal, 713206, India.

* Corresponding author;

E-mail: dipankar.sukul@gmail.com; Tel: +91 9434788066

hydrolysate contain different amino acid sequences. Major amino acid residues present in corn gluten protein fraction are glutamic acid, proline and leucine; other amino acids being present in minor percentages.²⁸ The pursuit to explore possible alternative uses this important co-product of plant processing industry has prompted us to undertake the current study.

Experimental

Metal coupons preparation and chemicals

Test specimens are cut from a commercially available mild steel rod (wt% composition: 0.24 C, 0.40 Si, 0.90 Mn, 0.07 Ni, 0.03 Cr, 0.01 P, 0.005 S and the remainder iron). The cross sectional surface is ground with different grade emery papers (400, 600, 800 and 1200), and washed thoroughly before using it as the working electrode in electrochemical measurements. Gluten hydrolysate from maize (Sigma-Aldrich) is used as received. As the molecular weight of gluten hydrolysate (being a polypeptide of varied chain lengths) cannot be determined accurately due to its inherent molecular complexity, the concentration is expressed in terms of ppm by weight.

Electrochemical measurements

Potentiodynamic polarization and electrochemical impedance measurement are done by conventional three-electrode system (model: CHI 608D) consisting of mild steel working electrode (WE) with an exposed area of 1 cm², platinum as counter electrode and saturated calomel electrode (SCE) as reference. Before electrochemical tests, the WE is kept in the test solution (300 mL) for sufficient time for attainment of steady open circuit potential (OCP). Polarization experiment is done with a potential sweep rate of 30 mV per min for the potential range of ±200 mV from OCP. Corrosion current density (i_{corr}) is determined from the intercept of extrapolated cathodic and anodic Tafel lines at the corrosion potential (E_{corr}). The values of inhibition efficiency, $\eta_p(\%)$ are calculated from the following equation:

$$\eta_p(\%) = \frac{i_{\text{corr}} - i_{\text{corr(inh)}}}{i_{\text{corr}}} \times 100 \quad (1)$$

where, i_{corr} and $i_{\text{corr(inh)}}$ are the values of corrosion current density of uninhibited and inhibited specimens, respectively.

Electrochemical impedance (EIS) measurements are performed in the frequency range 10 mHz to 100 kHz with a.c. amplitude of ± 5 mV at the rest potential. Nyquist plots obtained show only one time constant corresponding to one capacitive loop

without any trace of inductive loop at low frequency range. Observed capacitive loops are depressed with centre under the real axis, which may be interpreted in terms of microscopic roughness of the electrode surface and inhibitor adsorbed on it.^{29,30} Accordingly, these are fitted using an equivalent circuit consisting of parallel combination of polarization resistance-constant phase element, which is in series with solution resistance, $R_s[R_p\text{-}CPE]$ (Fig. S1 in in supplementary section).²⁹⁻³³ The impedance of CPE was given by

$$Z_{\text{CPE}} = Q^{-1} (i\omega)^{-n} \quad (2)$$

Q is an indicative parameter proportional to the capacitance of the double layer formed at the metal surface for $0 < n < 1$. For whole numbers of $n = 1, 0, -1$ CPE is reduced to the classical lumped elements capacitor (C), resistance (R), and inductance (L), respectively. To correlate the polarization resistance (R_p comprises charge transfer resistance along metal-electrolyte interface, resistance due to adsorbed inhibitor layer as well as corrosion products) and the double layer capacitance (C_{dl}) among the metal-solution interface, the later has been recalculated using the equation:^{31,32}

$$C_{\text{dl}} = (Q.R_p^{1-n})^{1/n} \quad (3)$$

The percentage inhibition efficiencies $\eta_z(\%)$ in terms of R_p are calculated through the following equation:

$$\eta_z(\%) = \frac{R_p - R_p^0}{R_p} \times 100 \quad (4)$$

Weight loss measurements

For weight loss measurement, polished, dried and accurately weighed rectangular mild steel coupons ($2.5 \times 2.5 \times 0.1$ cm³) are immersed in 1 M HCl (75 mL) without and with various concentration of inhibitor for a duration of 6h at different temperatures (293, 303, 313, 323K). After removing, loosely bound corrosion products are removed using a bristled brush, then washed thoroughly with distilled water and acetone and dried in a vacuum desiccator, and weighed. Corrosion rate (CR) is determined in terms of weight loss (in mg) per unit surface area (in cm²) per hour of immersion time. Percentage inhibition efficiency, $\eta_w(\%)$ is calculated following the relation:

$$\eta_w(\%) = \frac{CR_0 - CR}{CR_0} \times 100 \quad (5)$$

where, CR_0 and CR are the corrosion rate of metal coupons in acid medium without and with inhibitor. $\eta_W(\%)$ is a measure of the degree of surface coverage (θ) as per the relation:¹⁵⁻²¹

$$\theta = \eta_W(\%) / 100 \quad (6)$$

Surface analysis

Scanning electron microscope (SEM, S-3000N, Hitachi) is used to study the surface morphology of metal surface after immersion in 1 M HCl without and with inhibitor for a duration of 6h. The surface of the dried specimen is scratched with a knife and the resultant powder is then used for FTIR studies (KBr pellet method, Thermo Nicolet, model iS10).

Results and discussion

Polarization measurements

From potentiodynamic polarization plots and corresponding electrochemical parameters, it is seen i_{corr} decreases gradually with increase in concentration of gluten hydrolysate at a fixed temperature (Fig. 1 and Table 1). For all concentrations, i_{corr} increases with temperature (Fig. S2 in supplementary section), which is in agreement with Arrhenius theory for thermally induced reactions.

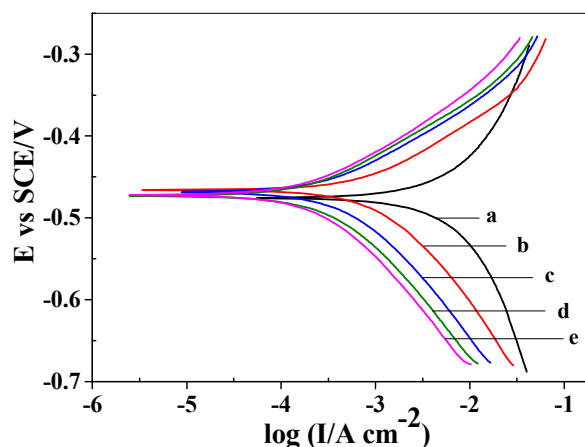


Fig. 1 Potentiodynamic polarization curves for mild steel in 1 M HCl in presence of (a) no inhibitor, (b) 100 ppm, (c) 250 ppm, (d) 500 ppm and (e) 1000 ppm gluten hydrolysate at 313K.

Both cathodic and anodic current in presence of inhibitor are lower for the whole potential range with respect to those observed in the blank solution (Fig. 1). Any substantial or regular variation for corrosion potential with inhibitor concentration is not seen; variation being limited within a relatively narrow range of ± 20 mV (Fig. 1 and Table 1). Cathodic and anodic Tafel slopes (b_c and

b_a , respectively) also do not indicate any systematic change. All these observations clearly indicate towards mixed-type corrosion inhibition behavior of gluten hydrolysate for mild steel in acid.⁵ This proposes a mechanism for corrosion inhibition comprising the blocking of both the cathodic and anodic active sites by the inhibitor molecules and thereby decreasing the rate

Table 1 Data from polarization studies for mild steel in 1 M HCl in various concentrations of gluten hydrolysate in different temperatures.

Temp. (K)	Inhibitor conc. (ppm)	$-E_{\text{corr}}$ (mV/SCE)	i_{corr} ($\mu\text{A cm}^{-2}$)	β_a (mV dec ⁻¹)	$-\beta_c$ (mV dec ⁻¹)	$\eta_{\%P}$
293	Blank	494	1260	74.0	100	-
	100	484	228	72.0	89.0	82.0
	250	478	112	68.0	94.0	91.0
	500	481	100	67.5	91.0	92.0
	1000	474	89.7	74.5	91.0	92.8
303	Blank	480	1760	76.0	91.0	-
	100	484	299	72.0	82.0	83.0
	250	470	132	62.5	85.4	92.5
	500	470	126	64.5	84.7	92.8
	1000	486	112	68.5	80.0	93.6
313	Blank	476	3160	91.0	102	-
	100	466	495	59.0	77.0	84.3
	250	469	218	60.0	72.0	93.1
	500	473	148	56.0	73.0	95.3
	1000	472	121	57.0	71.4	96.2
323	Blank	478	3310	83.0	93.4	-
	100	456	796	60.0	70.0	76.0
	250	459	532	56.5	75.0	84.0
	500	467	302	59.0	86.0	90.8
	1000	477	263	60.0	72.0	92.0

of both cathodic hydrogen evolution and anodic metal dissolution reactions. Within the range of temperature selected for the study, it

is observed that $\% \eta_p$ initially increases with temperature, becomes maximum at around 313K and then decreases.

Electrochemical impedance measurements

Nyquist plots, derived from EIS experiment, for mild steel in HCl solution in presence of different concentrations of gluten hydrolysate at a fixed temperature and those corresponding to different temperature at a particular concentration are shown in Figs. 2 and S3 (in supplementary section), respectively.

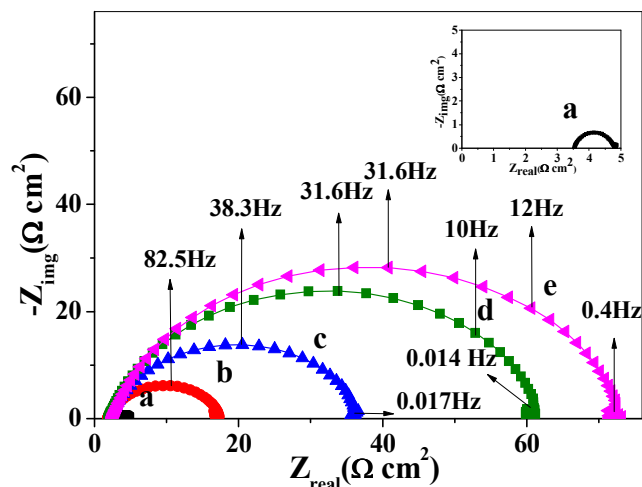


Fig. 2 Nyquist plots for mild steel in 1 M HCl in presence of (a) no inhibitor, (b) 100 ppm, (c) 250 ppm, (d) 500 ppm and (e) 1000 ppm gluten hydrolysate at 313K.

Using the equivalent circuit, as described in electrochemical measurements section, the corresponding fitting parameters and the inhibition efficiencies, $\eta_z(\%)$ obtained from the R_p values are tabulated in Table 2. Bode plots for mild steel in HCl in presence of 1000 ppm inhibitor at different temperatures are shown in Fig. 3.

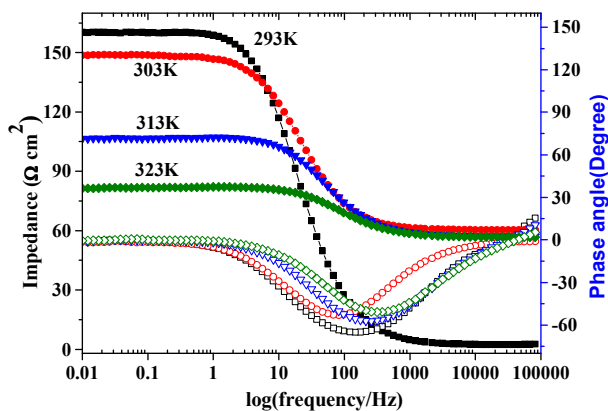


Fig. 3 Bode plots for mild steel in 1M HCl in presence of 1000 ppm gluten hydrolysate at different temperatures.

These clearly show the existence of only one time constant having one negative deflection in Bode magnitude plots. This validates the selection of the equivalent circuit as described. Nyquist plots and corresponding fitted parameters suggest that for all the temperatures, increasing inhibitor concentration provides increased diameter of the capacitive loop, which, in-turn, results in higher polarization resistance with concomitant decrease in Q or C_{dl} values. This is consistent with the model that inhibitor

Table 2 Impedance parameters for the corrosion of mild steel in 1 M HCl in various concentrations of gluten hydrolysate in different temperatures.

Temp. (K)	Inhibitor Conc. (ppm)	R_p (Ω cm^2)	Q ($\mu\Omega^{-1}$ s^n cm^2)	n	C_{dl} (μF cm^2)	$\eta_z(\%)$
293	Blank	5.3	904	0.86	378.0	
	100	42.3	205	0.86	95.0	87.5
	250	98.6	150	0.87	80.0	94.6
	500	139.0	130	0.87	71.3	96.2
	1000	159.0	128	0.86	67.8	96.6
303	Blank	3.6	978	0.85	360.0	
	100	32.0	190	0.87	88.5	88.7
	250	59.0	155	0.88	81.7	93.9
	500	98.0	140	0.86	69.6	96.3
	1000	125.0	120	0.88	67.6	97.1
313	Blank	1.7	1253	0.86	460.0	
	100	15.3	268	0.88	126.0	88.9
	250	34.0	255	0.85	110.0	95.0
	500	59.0	170	0.85	75.5	97.1
	1000	70.0	133	0.86	62.1	97.6
323	Blank	1.1	2108	0.82	558.0	
	100	9.0	371	0.83	115.0	87.7
	250	15.8	280	0.85	107.0	93.0
	500	28.0	238	0.86	105.0	96.0
	1000	35.0	191	0.83	69.0	96.8

molecules get adsorbed on the metal surface, resulting a resistive layer towards charge transfer. With gradual increment of inhibitor concentration, degree of surface coverage on the metal, as well as thickness of the

inhibitive layer enhances and as a consequence, R_p and $\% \eta_z$ values are found to increase, while Q or C_{dl} decreases. At a fixed inhibitor concentration, diameter of the capacitive loops decreases with increase in temperature. This suggests that at higher temperature, degree of surface coverage by the inhibitor molecules diminishes. This, in-turn is reflected in $\% \eta_z$ values, which shows that gluten hydrolysate to provide most efficient protective layer on metal surface at around 313K, above which its efficiency drops.

Weight loss measurement

Observations found from electrochemical measurements are verified by weight loss method. Rate of corrosion (CR) in terms of weight loss is also found to decrease with increase in gluten hydrolysate concentration (Table 3). For all the concentrations of

Table 3 Corrosion parameters from weight loss measurement for mild steel after 6h of immersion in 1M HCl.

Temp. (K)	Inhibitor conc. (ppm)	CR ($\text{mg cm}^{-2} \text{h}^{-1}$)	η_w (%)	θ
293	Blank	0.852	-	-
	100	0.094	88.9	0.89
	250	0.074	91.3	0.91
	500	0.068	92.0	0.92
	1000	0.053	93.8	0.94
303	Blank	1.834	-	-
	100	0.160	91.4	0.91
	250	0.136	92.6	0.93
	500	0.121	93.4	0.93
	1000	0.110	94.0	0.94
313	Blank	4.320	-	-
	100	0.320	92.6	0.93
	250	0.272	93.7	0.94
	500	0.222	94.8	0.95
	1000	0.185	95.7	0.96
323	Blank	5.664	-	-
	100	0.700	87.6	0.88
	250	0.680	88.0	0.88
	500	0.506	91.0	0.91
	1000	0.420	92.6	0.93

gluten hydrolysate used for the present study, it is observed that $\% \eta_w$ calculated from CR values initially increases upto 313K, and thereafter it tends to decrease (Fig. S4 in supplementary section).

Looking into the effect of time of exposure, it is seen that gluten hydrolysate at a concentration of 1000 ppm and at room temperature of around 303K, can provide good corrosion inhibition for nearly 50h of exposure (efficiency > 90%) in 1M HCl medium (Fig. 4). Corresponding data is shown in the table S1 (in the supplementary section). This supports the conclusion that gluten hydrolysate getting adsorbed on the metal surface, renders good

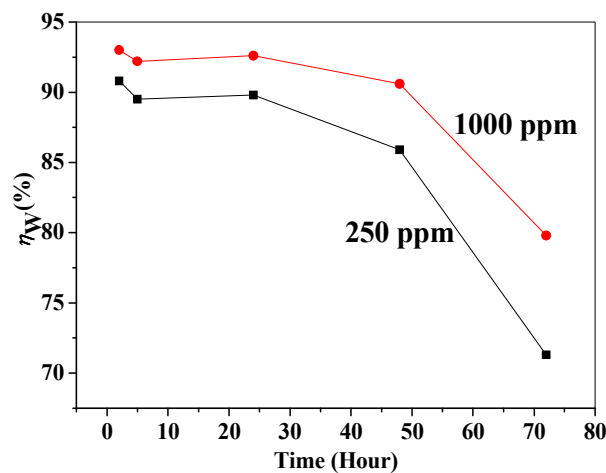


Fig. 4 Effect of exposure time on corrosion inhibition efficiency of gluten hydrolysate for mild steel in 1M HCl at around 303K.

corrosion protective layer and that lasts for considerable time of exposure in aggressive environment. After nearly 50h of exposure, inhibition efficiency begins to drop sharply. This may be due to breaking of amide linkages in protein chains due to hydrolysis in strong acidic environment, and thereby decreasing the molecular volume. This type of behaviour is seen for most of the biopolymeric corrosion inhibitors.²⁰ It may be mentioned here that most of the popular organic corrosion inhibitors (like N and S containing heterocyclic organic molecules) also provide comparable extent of inhibition efficiency for mild steel in 1M HCl, but the efficiency is maintained for more than 90h of exposure time.³³

Adsorption isotherm and adsorption parameters

Among several adsorption isotherms, Langmuir adsorption isotherm is found to be best suited to determine the adsorption characteristics of gluten hydrolysate on mild steel in acid medium and to evaluate corresponding thermodynamic parameters of adsorption. As per the model, the degree of surface coverage θ , as

determined from weight loss measurement, is related with concentration of the inhibitor (C) following the relation:³⁴

$$C/\theta = 1/K_{\text{ads}} + C \quad (7)$$

where, K_{ads} is constant of adsorption. For all the temperatures, excellent linear fitting of the experimental data points (correlation coefficient, $R^2 = 0.999$, and slope value within the range 1.04-1.07) confirms the applicability of the model (Fig. 5).¹⁹⁻²¹ From the values of the adsorption constant, K_{ads} , the standard free energy of adsorption (ΔG_{ads}^0) in different temperatures are determined using the following equation:¹⁹⁻²¹

$$\Delta G_{\text{ads}}^0 = -RT \ln(1 \times 10^6 K_{\text{ads}}) \quad (8)$$

where, 1×10^6 is the concentration of water molecules expressed in mg L^{-1} , R is the universal gas constant and T be the temperature.

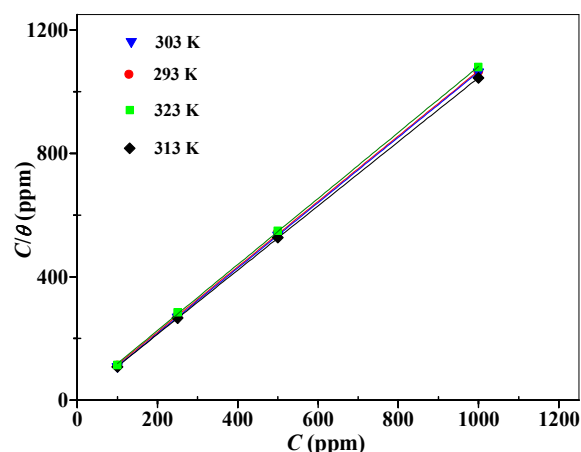


Fig. 5 Langmuir adsorption plot for mild steel in 1M HCl in presence of gluten hydrolysate at different temperatures.

Negative values of ΔG_{ads}^0 suggest spontaneous adsorption of gluten

Temp. (K)	Slope	R^2	K_{ads} (L mg^{-1})	$-\Delta G_{\text{ads}}^0$ (kJ mol^{-1})
293	1.06	0.9999	1.1×10^{-1}	28.27
303	1.06	0.9999	2.26×10^{-1}	31.05
313	1.04	0.9999	1.74×10^{-1}	31.40
323	1.07	0.9998	8.15×10^{-2}	30.37

hydrolysate on the metal at all the temperatures (Table 4).

Table 4 Calculated parameters from Langmuir Adsorption Isotherm

It is observed from the table that ΔG_{ads}^0 is progressively becoming more negative with increase in temperature and achieves a maximum negative value at 313K, above which it becomes less negative. Extent of adsorption of gluten hydrolysate is thus found to be temperature dependent. This type of temperature dependency cannot be explained on the basis of only physical or chemical mode of adsorption. Rather, it will be more logical to conclude that both types of adsorption plays there role during adsorption process over the whole temperature range.³⁵⁻³⁷

In order to elucidate more intricately on the adsorption characteristics in terms of enthalpy and entropy of adsorption, ΔG_{ads}^0 is plotted against T (Fig. 6). ΔH_{ads}^0 and ΔS_{ads}^0 can be evaluated from the intercept and slope, respectively, from the basic thermodynamic relation:

$$\Delta G_{\text{ads}}^0 = \Delta H_{\text{ads}}^0 - T \Delta S_{\text{ads}}^0 \quad (9)$$

Very interesting observation is found from the plot of ΔG_{ads}^0 vs T .

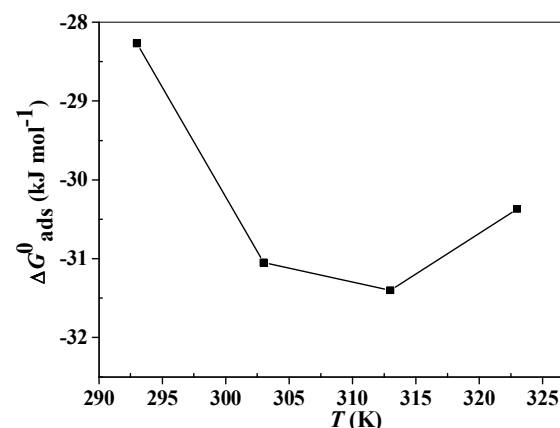


Fig. 6 Variation of free energy of adsorption with temperature

At lower temperature range (within 293-303K), ΔH_{ads}^0 is positive (around 53.1 kJ mol^{-1}), indicating adsorption to be endothermic. ΔS_{ads}^0 is also found to be positive (around 278 J mol^{-1}). These values suggest that at lower temperature range, adsorption is entropy driven, rather enthalpy driven. Also, due to endothermic nature, extent of adsorption initially increases with increase in temperature, which is reflected into ΔG_{ads}^0 values as well as inhibition efficiency. But at higher temperature range, ΔH_{ads}^0 , as well as ΔS_{ads}^0 are found to become negative ($-63.6 \text{ kJ mol}^{-1}$ and -103 J mol^{-1} , respectively, in the temperature range 313-323K). This shows that at higher temperature adsorption becomes exothermic, and essentially enthalpy driven.

Kinetics of adsorption and activation parameters

Kinetic-thermodynamic parameters have been evaluated following the variation of corrosion rate (CR) with temperature and employing the Arrhenius equations:

$$\log CR = \log \lambda - \frac{E^*}{2.303 RT} \quad (10)$$

$$CR = \frac{RT}{N_A h} \exp\left(\frac{\Delta S^*}{R}\right) \exp\left(\frac{-\Delta H^*}{RT}\right) \quad (11)$$

where E^* is the activation energy of the corrosion process, λ is the Arrhenius frequency factor (pre-exponential factor), R is the

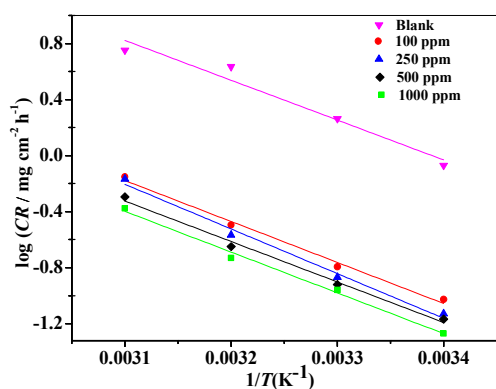


Fig. 7 Arrhenius plots for mild steel in 1M HCl solution in absence and presence of different concentrations of gluten hydrolysate.

universal gas constant, h is the plank's constant, N_A is Avogadro's number, T is the absolute temperature, ΔS^* is the entropy of activation and ΔH^* is enthalpy of activation. E^* and λ are determined from the slope and intercept, respectively, of the plot $\log CR$ vs $1/T$ (Fig. 7, Table 5). It is seen that rate of corrosion increases with increase in temperature, following Arrhenius equation. E^* values calculated in presence of the inhibitor with

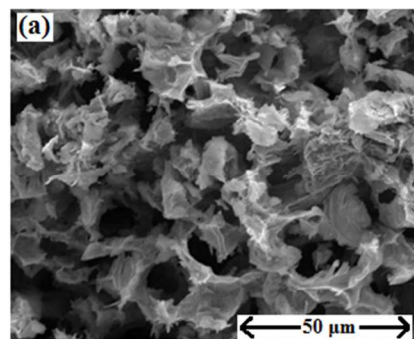
Table 5 Activation parameters for the mild steel dissolution in 1 M HCl in the absence and presence of gluten hydrolysate.

Conc (ppm)	λ ($\text{mg cm}^{-2} \text{h}^{-1}$)	E^* (kJ mol^{-1})	ΔH^* (kJ mol^{-1})	ΔS^* ($\text{kJ mol}^{-1} \text{K}^{-1}$)
Blank	42.46×10^8	53.88	51.63	-69.82
100	7.69×10^8	55.98	53.21	-84.11
250	47.20×10^8	61.02	58.27	-68.89
500	4.27×10^8	55.32	52.44	-89.28
1000	4.27×10^8	55.66	53.17	-88.41

various concentrations are seen to be greater than that for the blank solution. This illustrates the formation of a protective layer of the inhibitor on the metal surface, and thereby increasing the inhibition efficiency.³²⁻³⁴ But, apparent activation energy does not show any gradual variation with concentration of the inhibitor. Initially it increases, reaching a maximum value for 250 ppm, and then it decreases. Generally speaking, increasing activation energy corresponds to physical adsorption, whereas, decrease in activation energy can be related to chemical adsorption.³⁵⁻³⁷ Thus in the lower concentration range, extent of physical adsorption increases with gradual increase in concentration, leading to an increase in inhibition efficiency. This is reflected in an increase in E^* . But above 250 ppm, possibility of chemical adsorption becomes more dominating. Observation that above 250 ppm, inhibition efficiency increases even for a decrease in E^* , can be accounted for by the corresponding decrease in Arrhenius frequency factor (pre-exponential factor, λ). Enthalpy of activation (ΔH^*) and entropy of activation (ΔS^*) are evaluated from the slope and intercept, respectively, of the plot of $\log(CR/T)$ vs $(1/T)$ (Fig. S5 in supplementary section) and tabulated in table 5. It is seen that ΔH^* also varies in the same fashion as that for E^* . It is also observed that the difference between E^* and ΔH^* , on an average, remains very close to the average value of RT (2.56 kJ mol^{-1}).

Surface analysis

Corrosion inhibition potentiality of gluten hydrolysate is directly assessed by comparing the surface morphology of the mild steel sample immersed in 1 M HCl solution without and with 500 ppm of gluten hydrolysate through scanning electron micrographs (SEM) of the metal surface (Figs. 8a and b). Mild



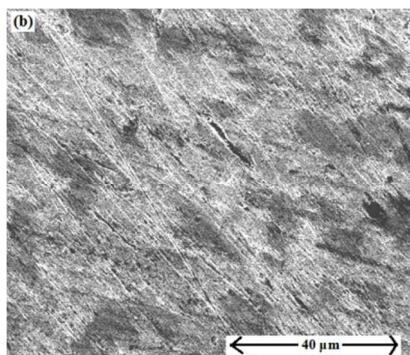


Fig. 8 SEM images of mild steel after immersion in 1M HCl having (a) no inhibitor (b) Gluten hydrolysate.

steel surface immersed in HCl shows a very rough surface due to formation of corrosion product. But in presence of gluten hydrolysate, a much clean and smooth surface comparable with that of polished one is observed. This provides conclusive evidence towards the ability of gluten hydrolysate in decreasing the aggressiveness of HCl in regard to its corrosive characteristics for mild steel.

Formation of corrosion inhibitive layer on the mild steel surface is further confirmed by comparing the FTIR spectra of gluten hydrolysate (Fig.9A) with that of the adsorbed surface layer of mild steel immersed in 1 M HCl having 1000 ppm gluten hydrolysate (Fig.9B). The main absorption bands of polypeptides or proteins are due to their characteristic amide I (mainly stretching vibration of the C=O group) at around 1660 cm^{-1} and amide II (in-plane N-H bending) at nearly 1585 cm^{-1} .³⁸⁻⁴⁰ These bands can distinctly be seen in the FTIR spectrum of gluten

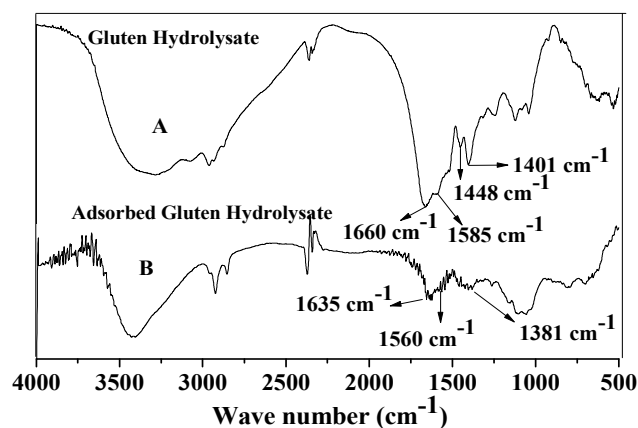


Fig. 9. FTIR spectra of gluten hydrolysate in (A) native form, and (B) surface adsorbed form.

hydrolysate (Fig. 9A). The presence of a bands at 1448 and 1401 cm^{-1} are due to C-N stretching and COO^- vibrations, respectively, of different amino acid side chains present in gluten hydrolysate.^{39,40} Amide A band ($\sim 3300\text{ cm}^{-1}$) and amide B ($\sim 3100\text{ cm}^{-1}$) bands originate from a Fermi resonance between the first overtone of amide II and the N-H stretching vibrations.³⁹ Bands in the range of 2961 cm^{-1} to 2868 cm^{-1} are due to aliphatic C-H stretching vibrations.^{39,40} In surface adsorbed gluten hydrolysate, amide I band is prominently red shifted to 1635 cm^{-1} . Amide II band at 1585 cm^{-1} in native gluten hydrolysate is also shifted to 1560 cm^{-1} (Fig. 9B). This illustrates the participation of amide groups in the polypeptide (protein) backbone towards adsorption of proteins on metal surface. Absorption bands at 1448 and 1401 cm^{-1} are also seen to undergo prominent shift towards lower wavenumber region with some broadening of the bands in the adsorbed state. Thus in conjunction to amide group, involvement of side chains present in different amino acid residues can definitely be argued during whole adsorption process.

Discussion

Observations from electrochemical as well as weight loss techniques have shown that inhibition efficiency of gluten hydrolysate towards corrosion of mild steel in HCl medium does not vary monotonically with temperature, it first gradually increases from lower temperature, reaching a maximum value at around 313 K , and then decreases. Free energy of adsorption is also found to be temperature dependent. Activation energy for adsorption process, on the other hand, depends on concentration. These observations, along with the findings from FTIR studies suggest the possible mode of interaction between gluten hydrolysate with mild steel surface in acid medium comprising of competition between electrostatic physical and chemical adsorption model as a function of temperature and concentration, as well as complex nature of adsorption of polypeptide chains of protein on metal surface.⁴¹⁻⁴⁴ It is well established that mild steel surface in 1 M HCl media under equilibrium condition carries net positive charge. Hence, it is understood that at least a fraction of the metal surface should be pre-occupied by the Cl^- ions.^{13,35} On the other hand, it is most possible that some of the peptide chains remain in protonated form in acid medium. Thus at lower concentration and lower temperature range, electrostatic physical adsorption of protonated peptide chains on the metal surface through Cl^- ions can be considered as a natural phenomenon.

Even, at very lower temperature, formation multilayer cannot be ruled out (i.e., physical adsorption leading to multilayer formation at lower temperature). In these cases, electrostatic repulsion among the charged groups present in the adjacent peptide chains can result into increase in enthalpy (endothermic).³⁵⁻³⁷ Such repulsive interaction as well as possibility of multilayer formation can be responsible for positive entropy of adsorption. Additionally, release of the water molecules which were bound on the metal surface before adsorption the peptide chains of protein, can also contribute towards positive ΔS_{ads}^0 .⁴¹⁻⁴³ Possibility of physical adsorption remains predominant nearly up to 250 ppm and at a result E^* becomes maximum at this point. At higher concentration, more number of reactive functional groups is available for adsorption. Higher temperature also opens up the protein chains and thus enhancing the accessibility of such groups.⁴³ These reactive centers with either lone pair of electrons or negative charge present on them (e.g. COO⁻ group present in glutamic acid) can directly interact with the adsorption sites on metal which are not occupied by Cl⁻ ions, or even by replacing those pre-adsorbed Cl⁻ ions, through charge transfer mechanism. Data from FTIR studies suggest the occurrence of such interaction. As a result, heat is evolved (exothermic chemisorption), as well as ΔS_{ads}^0 becomes negative. As chemisorption becomes more dominating over physisorption, E^* is seen to decrease gradually beyond 250 ppm concentration. Entropy of activation (ΔS^*) for all the inhibitor concentration remains more negative than that in the blank, except for 250 ppm concentration. It may be explained following the formation of compact inhibitor layer on the metal surface at the activated state, thus lowering the disorderness of that state. For 250 ppm concentration, possible multilayer formation or/and enhanced repulsive interaction among adjacent peptide chains can be responsible for slight increase in the disorderness of the activated state compared that that in the blank solution. It is noteworthy that gluten hydrolysate does not impart inhibition of corrosion of mild steel in 3.5% aqueous NaCl solution (pH ~6) to any significant extent. At this pH, it is very much unlikely that the peptide side chains will acquire positive charges. As a result, electrostatic repulsion among the surface adsorbed Cl⁻ ions and the lone pair of electrons of peptide bonds as well as negative charge present on glutamic acid residue provides hindrance towards close approach between the peptide chain and the metal surface required for any possible charge transfer leading to surface adsorption and

subsequent corrosion inhibition. This further supports our explanation regarding the nature of adsorption and inhibition property of gluten hydrolysate towards corrosion of mild steel in highly acidic medium.

Conclusions

Gluten hydrolysate is shown to act as an efficient green inhibitor in mitigating corrosion of mild steel in 1M HCl. High inhibition potentiality is observed (more than 90% with 1000 ppm of concentration) in a temperature range of 293 to 323K and that for considerable time of exposure. Potentiodynamic polarization studies indicate gluten hydrolysate to behave as a mixed-type corrosion inhibitor for mild steel in acid medium. Results from EIS and weight loss experiments can be best explained following formation of corrosion resistive layer of the gluten hydrolysate on the metal surface. Inhibition efficiency is found to increase initially upto 313K and then it falls down. Thermodynamic adsorption parameters are seen to be dependent on temperature, while activation parameters are concentration dependent. A model of simultaneous physical and chemical adsorption depending on temperature and concentration has been put forward to explain the experimental findings. FTIR studies confirm the involvement of amide groups as well as amino acid side chains for adsorption of gluten hydrolysate on metal surface.

Acknowledgements

DS thanks Department of Science and Technology, Govt. of India for supporting a research project under Fast Track Scheme for Young Scientists (no. SR/FT/CS-110/2010, dt. 20.09.2011).

References

- 1 M. B. P. Mihajlović and M. M. Antonijević, *Int. J. Electrochem. Sci.*, 2015, **10**, 1027.
- 2 M. Finšgar and J. Jackson, *Corros. Sci.*, 2014, **86**, 17.
- 3 P. Rajeev, A. O. Surendranathan and C. S. N. Murthy, *J. Mater. Environ. Sci.*, 2012, **3**, 856.
- 4 K. Sayin and D. Karakaş, *Corros. Sci.*, 2013, **77**, 37.
- 5 I. L. Rozenfeld, *Corrosion Inhibitors*, McGraw-Hill Inc, New York, 1981.
- 6 S.A. Abd El-Maksoud, *Int. J. Electrochem. Sci.*, 2008, **3**, 528.
- 7 D. M. Bastidas, E. Cano and E. M. Mora, *Anti-Corros. Meth. Mater.*, 2005, **52**, 71.
- 8 V.S. Saji, *Recent Patents on Corros. Sci.*, 2011, **1**, 63.

- 9 L. Bai, L. -J. Feng, H. -Y. Wang, Y. -B. Lu, X. - W. Lei and F. -L. Bai, *RSC Adv.*, 2015, **5**, 4716.
- 10 P. B. Raja and M. G. Sethuraman, *Mater. Lett.*, 2008, **62**, 113.
- 11 S. A. Umoren, *The Open Corros. J.*, 2009, **2**, 175.
- 12 B. E. A. Rani and B. B. J. Basu, *Int. J. Corros.*, 2012, doi:10.1155/2012/380217.
- 13 Md. A. Amin, K. F. Khaled, Q. Mohsen and H. A. Arid, *Corros. Sci.*, 2010, **52**, 1684.
- 14 M. Li, J. Xu, R. Li, D. Wang, T. Li, M. Yuan and J. Wang, *J. Colloid. Inter. Sci.*, 2014, **417**, 131.
- 15 R. Solmaz, *Corros. Sci.*, 2014, **81**, 75.
- 16 R. S. A. Hameed, E. A. Ismail, A. H. Abu- Nawwas and H. I. Al-Shafey, *Int. J. Electrochem. Sci.*, 2015, **10**, 2098.
- 17 F. Zhang, J. Pan and P. M. Claesson, *Electrochim. Acta*, 2011, **56**, 1636.
- 18 S. A. Umoren, U. M. Eduok, A. U. Israel, I. B. Obot and M. M. Solomon, *Green Chem. Lett. Rev.*, 2012, **5**, 303.
- 19 P. Roy, A. Pal and D. Sukul, *RSC Adv.*, 2014, **4**, 10607.
- 20 P. Roy, P. Karfa, U. Adhikari and D. Sukul, *Corros. Sci.*, 2014, **88**, 246.
- 21 P. Roy and D. Sukul, *RSC Adv.*, 2015, **5**, 1359.
- 22 P. R. Shewry, N. G. Halford, P. S. Belton and A. S. Tatham, *Phil. Trans. R. Soc. Lond. B*, 2002, **357**, 133.
- 23 L. Day, M. A. Augustin, I. L. Batey and C.W. Wrigley, *Trends in Food Sci. Tech.*, 2006, **17**, 82.
- 24 B. H. Sarmadi and A. Ismail, *Peptides*, 2010, **31**, 1949.
- 25 X. Zheng, L. Li, X. Liu, X. Wang, J. Lin and D. Li, *Appl. Microbiol. Biotechnol.*, 2006, **73**, 763.
- 26 E. Apper-Bossard, A. Feneuil, A. Wagner and F. Respondek, *Aquatic Biosystems*, 2013, **9**, 13 pages.
- 27 M. Funaba, Y. Oka, S. Kobayashi, M. Kaneko, H. Yamamoto, K. Namikawa, T. Iriki and Y. Hatano, M. Abe, *Can. J. Vet. Res.*, 2005, **69**, 299.
- 28 F. P. O'Mara, J. J. Murphy and M. Rath, *J. Anim. Sci.*, 1997, **75**, 1941.
- 29 T. Pajkossy, *Solid State Ionics*, 2005, **176**, 1997.
- 30 U. Rammelt and G. Reinhard, *Corros. Sci.*, 1987, **27**, 373.
- 31 M. Chevalier, F. Robert, N. Amusant, M. Traisnel, C. Roos and M. Lebrini, *Electrochim. Acta*, 2014, **131**, 96.
- 32 G. J. Brug, A. L. G. van den Eeden, M. Sluyters-Rehbach and J. H. Sluyters, *J. Electroanal. Chem.*, 1984, **176**, 275.
- 33 A. Dutta, S.K.. Saha, P. Banerjee and D. Sukul, *Corros. Sci.*, 2015, doi:10.1016/j.corsci.2015.05.065.
- 34 K.Y. Foo and B.H. Hameed, *Chem. Engg. J.*, 2010, **156**, 2.
- 35 E. A. Noor, *Int. J. Electrochem. Sci.*, 2007, **2**, 996.
- 36 A. Popova, *Corros. Sci.*, 2007, **49**, 2144.
- 37 A. Zarrouk, B. Hammouti, H. Zarrok, S. S. Al-Deyab and M. Messali, *Int. J. Electrochem. Sci.*, 2011, **6**, 6261.
- 38 M. Jackson and H. H. Mantsch, *Crit. Rev. Biochem. Mol. Biol.*, 1995, **30**, 95.
- 39 A. Barth, *Biochim. Biophys. Acta*, 2007, **1767**, 1073.
- 40 A. Barth, *Prog. Biophys. Mol. Biol.*, 2000, **74**, 141.
- 41 N. P. Cosman, K. Fatih and S. G. Roscoe, *J. Electroanal. Chem.*, 2005, **574**, 261.
- 42 S. Omanovic and S. G. Roscoe, *J. Colloid Inter. Sci.*, 2000, **227**, 452.
- 43 K. Nakanishi, T. Sakiyama and K. Imamura, *J. Biosci. Bioengg.*, 2001, **91**, 233.
- 44 O. Santos, T. Nylander, M. Paulsson and C. Trägårdh, *J. Food Engg.*, 2006, **74**, 468.